DOI: 10.1002/chem.200701994

A Core–Shell Nanoparticle Approach to Photoreversible Fluorescence Modulation of a Hydrophobic Dye in Aqueous Media

Jian Chen, Fang Zeng, Shuizhu Wu,* Qiming Chen, and Zhen Tong[a]

Abstract: Amphiphilic core–shell nanoparticles containing spiropyran moieties have been prepared in aqueous media. The nanoparticles consist of hydrophilic and biocompatible poly(ethyleneimine) (PEI) chain segments, which serve as the shell, and a hydrophobic copolymer of methyl methacrylate (MMA), a spiropyran-linked methacrylate, and a cross-linker, which forms the core of the nanoparticles. A hydrophobic fluorescent dye based on the nitrobenzoxadiazolyl (NBD) group was introduced into the nanoparticles to form NBD–nanoparticle complexes in water. The nanoparticles not only greatly enhance the fluorescence emission of the hydrophobic dye NBD in aqueous media, probably by accommodating the dye molecules in the interface between the hydrophilic shells and the hydrophobic cores, but also modulate the fluorescence of the dye through intraparticle energy transfer. This biocompatible and photoresponsive nanoparticle complex may find applications in biological areas such as biological diagnosis, imaging, and detection. In addition, this nanoparticle approach will open up possibilities for the fluorescence modulation of other hydrophobic fluorophores in aqueous media.

Keywords: chromophores · fluorescence · nanoparticles · polymers · spiro compounds

Introduction

Materials with properties that can be optically modulated are of high interest in a broad range of scientific fields, including biotechnology and advanced optics.[1–3] Fluorescence techniques are rapidly becoming a leading methodology in many biological diagnosis, imaging, and detection applications, primarily because of their versatility and ease of use. The modulation of fluorescence emission in aqueous media represents a new trend in the application of fluorescence in biological studies because it can be used to selectively highlight cells, organelles, or proteins.[4] Photochromic compounds such as spiropyran, which can be interconverted reversibly by light between two states with different spectroscopic properties, can be used to achieve photoreversible fluorescence modulation through energy transfer.[5] In recent years, various attempts have been made to enhance the fluorescence emission and achieve photoreversible fluorescence modulation of fluorophores in aqueous media, for example, by chemical modification of fluorophores to produce dyad or triad molecules.[6,7] However, the fluorophore moieties in the dyad or triad molecules still tend to aggregate in aqueous media, which usually leads to fluorescence quenching. In addition, they usually lack the necessary biocompatibility for applications in biotechnology.

Recently, fluorescent nanoparticles have attracted increasing attention as a result of their advantages over conventional dyes for labeling and sensing. They hold the most promise as three-dimensional scaffolds for the development of new tunable and versatile sensing devices because the selectivity and operating range can be monitored, without any synthetic effort, by changing the receptor and/or the dye. Hence, they are widely used as novel luminescent probes in biological and environmental fields.[8,9] The fluorescent nanoparticles are not only very bright and exhibit improved photostability, but also feature versatility in their design and synthesis. They can be prepared by incorporating fluorescent dyes into various quantum dots and nanoparticles by covalent linkage, entrapment, or self-assembly strategies.[10] Thus, the inclusion of fluorescent labels or probes within nanoparticles is an attractive strategy for the application of fluorescence techniques in aqueous systems. In many of the applications that involve the use of fluorescent nanoparticles, fluorescence resonance energy transfer (FRET), which is an

[a] J. Chen, Prof. F. Zeng, Prof. S. Wu, Q. Chen, Prof. Z. Tong
College of Materials Science and Engineering
South China University of Technology, Guangzhou 510640 (China)
Fax: (+86) 20-8711-4649
E-mail: shzhwu@scut.edu.cn

Supporting information for this article is available on the WWW under http://www.chemeurj.org/ or from the author.

attractive mechanism because it does not directly produce redox-active ions that could lead to photodamage or other undesirable processes, has been widely employed to realize the various functions that operate in, for example, sensors, probes,[11] optical switches,[12] and biological imaging.[13] In addition, FRET can be applied experimentally to characterize the nanoparticles.[14]

Among their various potential applications, fluorescent nanoparticles can be utilized for fluorescence modulation. Park and co-workers synthesized a new class of fluorescent and photochromic compounds and used one of these to form fluorescent nanoparticles that exhibited high-contrast on/off fluorescence switching properties upon UV/Vis irradiation.[9a] Very recently, Zhu et al. incorporated a spiropyran and a fluorescent dye into polymer nanoparticles to generate optically addressable two-color fluorescent systems, and they used light to change the color of the nanoparticles.[15]

Herein, we demonstrate a new strategy using a class of spiropyran-containing amphiphilic core–shell nanoparticles to realize photoreversible fluorescence modulation (Scheme 1). The nanoparticles can incorporate hydrophobic fluorescent dyes and reversibly switch their fluorescence emission upon UV or visible-light irradiation. In this way, various hydrophobic dyes can be easily incorporated into the nanoparticles without additional synthetic effort. In the nanoparticles, the hydrophilic and biocompatible poly(ethyleneimine) (PEI) chain segments act as the shell and a hydrophobic copolymer of methyl methacrylate (MMA), a spiropyran-linked methacrylate (SPMA), and a cross-linker forms the core of the nanoparticles. In this study, a hydrophobic fluorescent probe based on a hydrophobic nitrobenzoxadiazolyl dye (NBD)[16] was loaded onto the nanoparticles in aqueous media to form a photoswitchable fluorescent nanoparticle system. This fluorescent nanoparticle complex possesses several features.

First, the nanoparticles with PEI chain segments as the shell are hydrophilic and free from other surfactant molecules; the particle matrix can protect the biological environment (for example, the intracellular environment) from any toxic dyes. Branched PEI was used in this study because PEI is a well-studied and commercially available polyamine with defined molecular weights. Also, a series of nanoparticles could be obtained by choosing PEIs with different molecular weights. As a weak, polybasic aliphatic amine with a high concentration of amino groups, PEI has been widely used in the fields of biochemistry and medicine as a result of its unique features, such as its ability to bind to biomacromolecules. On the one hand, PEI can form complexes with biological substances and exert positive effects on the latter, for example, PEI as a polycation can interact with proteins through long-range coulombic forces and increase the stability of the proteins as well as enhance the rate of enzyme-catalyzed reactions.[17] Moreover, PEI can form polyplexes with DNA through covalent conjugation or coulombic interaction and thus enhance the transfection efficiency.[18] On the other hand, the interaction of PEI with proteins often leads to negative effects such as unspecific bindings[19] and, accordingly, cytosolic protein chemistry can interfere with the above-mentioned polyplexes.[20] Various measures have been taken to reduce or avoid these unspecific bindings, for example,[21] branched PEI and certain PEI derivatives can be used to avoid unspecific binding[21a] and a natural anionic mucopolysaccharide can be deposited onto the cationic surface of DNA–PEI complexes to recharge the surface potential and reduce the number of unspecific interactions with proteins.[21b] In this approach to nanoparticle preparation, many amine-containing water-soluble polymers can be used to initiate the formation of nanoparticles. Thus, the unmodified branched PEI used in this study, which may cause unspecific binding in biological applications, could eventually be replaced by other amine-containing polymers such as modified PEIs or other biomacromolecules so that the unspecific binding can be reduced or avoided.

Second, many dyes are hydrophobic and in aqueous media their fluorescence emission is very weak as a result of their poor solubility. Moreover, for those dyes that undergo photoinduced intramolecular charge transfer (ICT) upon excitation and emit fluorescence as a result of the charge recombination process,[22] high polari-

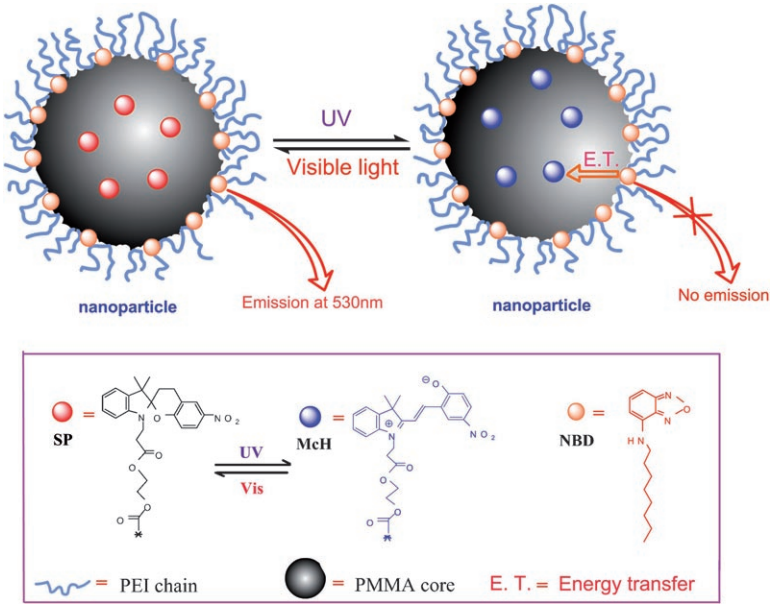

Scheme 1. Photoreversible fluorescence modulation of the NBD–nanoparticle complex.

ty solvents like water often shift the fluorescence spectra of those dyes strongly to the red.[22b,c] In addition, for dyes that can form hydrogen bonds with water molecules, hydrogen-bonding often leads to nonradiative dissipation of the excitation energy into hydrogen-bonding vibrations, and hence significantly quenches the fluorescence emission of the dyes.[23] Thus, for the strategy described herein, by solubilizing the hydrophobic fluorescent dyes and providing them with a hydrophobic environment, the amphiphilic core–shell nanoparticles not only retain the high fluorescence emission intensity of the dye, but also prevent the unfavorable effects of dye–water interactions. Moreover, this approach using amphiphilic nanoparticles can be applied to other hydrophobic fluorophores as the NBD dye herein can be readily replaced by other hydrophobic dyes without covalently connecting the dyes to the nanoparticles.

Finally, the nanometer size of the particles not only minimizes physical perturbation in biological substances, but also confines a considerable number of the fluorescent dye molecules (donor) and spiropyran moieties (acceptor) within the Förster radius. Thus the fluorescence of the former can be photoreversibly modulated by the latter through energy transfer.

The fluorescent dye/nanoparticle prepared in this study may find applications in biological diagnosis, imaging, and detection. For example, like the polymer nanoparticles prepared by Zhu et al.,[15] the amphiphilic core–shell nanoparticles can also be transported into cells by using liposomes as delivery vehicles and be used to highlight the cells; this highlighting of the cells can be controlled by light irradiation. In addition, for the detection (or diagnosis) of cancer cells, the nanoparticle complexes, with amine groups on their surfaces, can be readily conjugated (through covalent bonds or coulombic interactions) with a specific antibody to form bioconjugated nanoparticles (antibody-labeled nanoparticles) and can accordingly be used for the detection of cancer cells.

Results and Discussion

Amphiphilic nanoparticles with spiropyran moieties can accommodate a hydrophobic fluorescent dye in aqueous media, thereby enhancing its fluorescence emission. In addition, the nanoparticles can photoreversibly modulate the fluorescence emission of the incorporated hydrophobic dye, as illustrated in Scheme 1.

Preparation of amphiphilic spiropyan-containing nanoparticles: To synthesize nanoparticles with covalently linked spiropyran groups, we first synthesized SPCOOH, a carboxy-containing spiropyran, according to a literature procedure.[24] We obtained a spiropyran-containing methacrylate (SPMA) monomer by esterification of SPCOOH with 2-hydroxyethyl methacrylate (HEMA). The core–shell nanoparticles were prepared by a procedure similar to that previously reported by us[25] following a literature strategy,[26] except that an additional spiropyran-linked methacrylate (SPMA) monomer was used in the reaction and covalently incorporated into the nanoparticles. In this preparation, a water-soluble initiator, *tert*-butyl hydroperoxide (TBHP), was used to generate macromolecular free radicals by reacting with the amine groups in the PEI chains to initiate the polymerization of a mixture of methyl methacrylate (MMA)/acrylate-linked spiropyran (SPMA)/ethylene dimethacrylate (EDMA) in water, thereby forming a copolymer of PEI-*graft*-(MMA-*co*-SPMA-*co*-EDMA). As the copolymer of MMA, SPMA, and EDMA is hydrophobic, whereas the PEI chains remain hydrophilic, the amphiphilic copolymers consequently form the core–shell particles in water and the PEI chain segments the shell. The average diameters of the prepared core–shell particles are in the range of around 80–130 nm, depending on the PEIs used and the ratio of PEI to MMA. Specifically, for sample NP-A1, with a 1:4 weight ratio of PEI (M_w = 1800) to MMA, we can obtain a stable dispersion of nanoparticles with an average diameter of 82 nm, as determined by atomic force microscopy (AFM) and dynamic light scattering (DLS) (Figure 1). The average particle sizes of the samples determined by DLS are listed in Table 1.

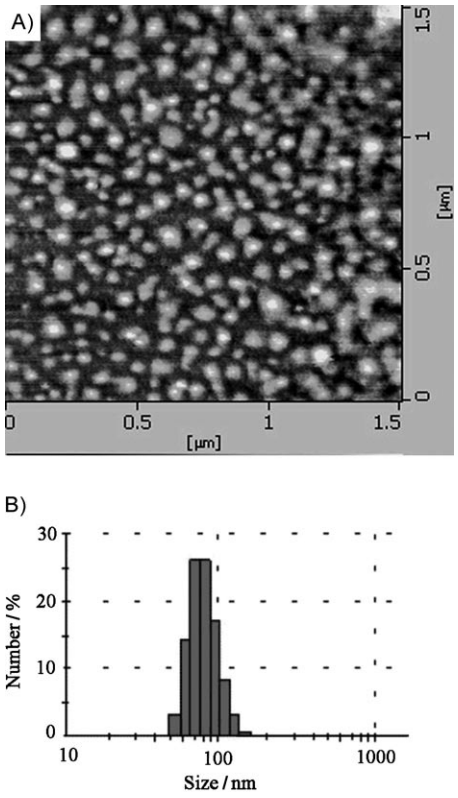

Figure 1. A) AFM image of spiropyran-containing nanoparticles (sample NP-A1). B) Size distribution for the same nanoparticle sample determined by light scattering.

The absorption spectra of spiropyran-linked methacrylate (SPMA) in toluene as well as the spiropyran-containing (spiropyran-doped) nanoparticles in water upon UV or visible-

Table 1. Spiropyran-containing nanoparticle samples prepared in this work.

Sample[a]	M_w of PEI[b]	SP feed [g]	Diameter (by DLS) [nm]
NP-A1	1800	0.10	82
NP-A2	1800	0.050	92
NP-A3	1800	0.025	86
NP-A4	1800	0.0125	97
NP-B1	10000	0.10	106
NP-B2	10000	0.050	104
NP-B3	10000	0.025	111
NP-C0	70000	0.00	123
NP-C1	70000	0.10	119
NP-C2	70000	0.050	116
NP-C3	70000	0.025	124

[a] The MMA and EDMA feeds are 3.0 and 0.03 g, respectively. [b] Weight ratio of PEI/MMA is 1:4.

light irradiation are shown in Figure 2. It is well known that spiropyran molecules can assume one of two stable states: The open-ring state, known as the protonated merocyanine (McH) form, and the closed-ring state, known as the spiro (SP) form. Upon irradiation with UV light, the spiropyran molecules adopt the McH form, whereas with visible light, they adopt the SP form.[3,27] Similarly, for the SPMA monomer, after visible-light irradiation, the spiropyran moieties assumed the SP form and exhibited no absorption band from 400 to 700 nm. However, after UV irradiation, a new absorption band at 580 nm appeared owing to the formation of the McH form, as shown in Figure 2A. The absorption behavior of the spiropyran-containing nanoparticles is similar to that of the methacrylate-linked spiropyran monomer (Figure 2B) except that, because of a light-scattering effect of the nanoparticles, the intensity of the absorption decreases from low wavelength to high wavelength. This absorption behavior of the amphiphilic nanoparticles indicates that the spiropyran-containing nanoparticles can also exhibit photochromic behavior in aqueous media.

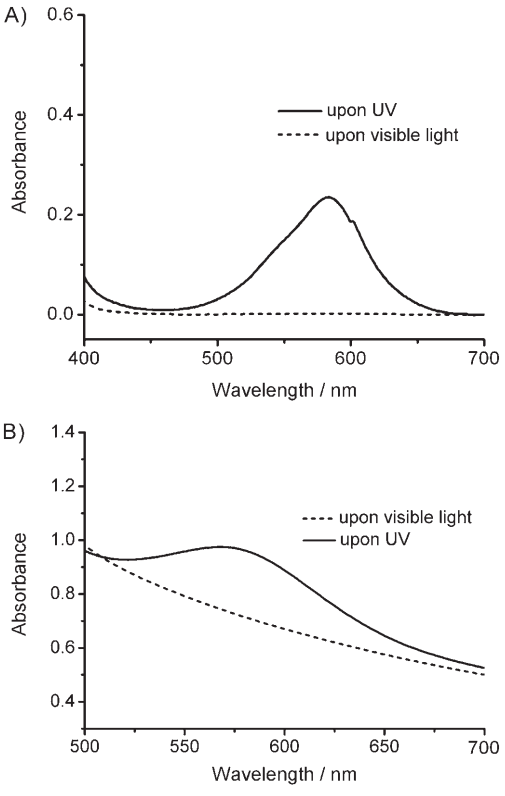

Figure 2. Absorption spectra of A) the spiropyran-linked methacrylate (SPMA) monomer in toluene and B) spiropyran-containing nanoparticles (sample NP-A3) in water with a solid content of 5.0 wt% upon UV or visible light irradiation. In panel B, the decrease in the absorption curves from short to long wavelength is due to the light scattering effect of particles in water.

Introduction of a hydrophobic fluorescent dye into spiropyran-containing nanoparticles: A fluorescent dye with a nitrobenzoxadiazolyl (NBD) group and a C_8 alkyl tail (structure is shown in Scheme 1) was synthesized and used in this study as the model hydrophobic dye. This NBD dye is hydrophobic as the nitrogen atom undergoes a strong electron-withdrawing effect from the nitrobenzoxadiazolyl group. Figures 3 and 4 show the absorption spectra and fluorescence emission of NBD in pure water and in nanoparticle

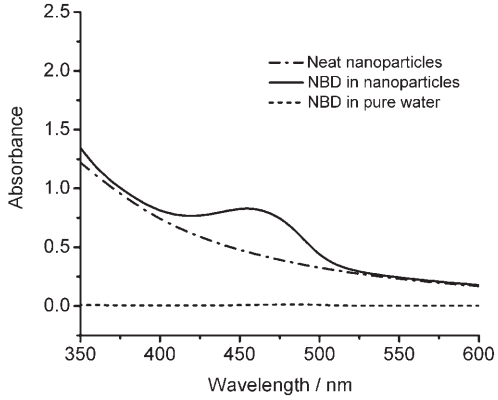

Figure 3. Absorption spectra of a saturated water solution of NBD, NBD in a nanoparticle dispersion (sample NP-C0), and the neat nanoparticle dispersion (sample NP-C0). To avoid interference of the absorption band by spiropyran moieties, no spiropyran monomer was incorporated into the nanoparticles.

dispersions, respectively. The NBD dye, owing to its hydrophobic nature, exhibits very low solubility in pure water. Its solution remains almost colorless with a very weak fluorescence emission at 541 nm (inset of Figure 4), and no reliable UV/Vis absorption spectrum could be obtained from its saturated water solution.

Although the NBD dye exhibits very low solubility in pure water, it can still be transferred to the spiropyran-doped nanoparticles from its solid state in water by stirring at 50 °C, as described in the Experimental Section. The amphiphilic nanoparticles acted like surfactant molecules and incorporated the hydrophobic dye molecules, thereby drastically increasing the solubility of the dye in the aqueous dis-

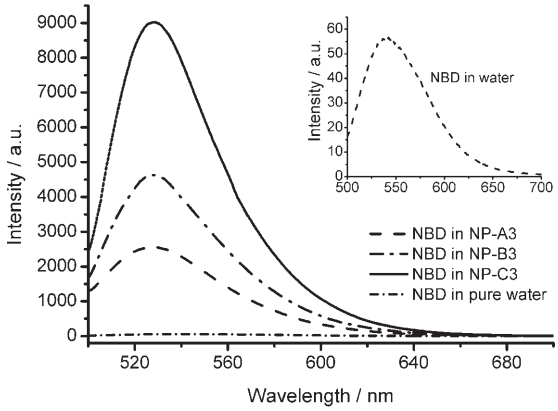

Figure 4. Fluorescence emission of the NBD dye in pure water and in water dispersions of different nanoparticles (excited at 490 nm). The fluorescence spectrum of NBD in pure water was recorded by using a saturated water solution of NBD. The solid content of the nanoparticle dispersions was 5.0 wt%. The NBD dye was added to these nanoparticle dispersions until the complexes reached their maximum emission intensity and the NBD concentrations (in water) were 1.07×10^{-5}, 1.89×10^{-5}, and 4.23×10^{-5} M in the NP-A3, NP-B3, and NP-C3 dispersions, respectively.

persion. As a result of the introduction of the dye into the nanoparticle, the NBD–nanoparticle dispersion exhibited a prominent absorption at around 470 nm (Figure 3). Moreover, the fluorescence intensity of the NBD–nanoparticle dispersion increased greatly (by ≈40–180 times) and a moderate blue shift of 8 nm was observed relative to that in pure water, as shown in Figure 4. The results indicate that the dye molecules were actually incorporated into the nanoparticles, and the strong fluorescence intensity of the dye suggests that the dye molecules reside in a more hydrophobic environment, in this case probably at the interface between the hydrophilic PEI shell and the hydrophobic PMMA/SPMA core.

In this study, we used three different nanoparticle samples to accommodate the hydrophobic dye. To test the accommodating capacity of the different nanoparticles, we gradually increased the amount of NBD dye during complex formation until the emission intensity of the complexes reached a maximum. It can be seen in Figure 4 that the fluorescence emissions of the NBD dye in the three nanoparticle dispersions have different intensities. For the three nanoparticle samples (NP-A3, NP-B3, and NP-C3), the one with PEI chains of the highest molecular weight could incorporate more NBD molecules and the higher intensity at the maximum emission wavelength was due to the higher amount of NBD incorporated into the core–shell interface of the nanoparticles as the fluorescence intensities were not normalized to the corresponding optical density at the excitation wavelength of the solutions. However, the reason for this fluorescence dependence on the PEI molecular weight is presently unclear.

Photoreversible modulation (switching) of fluorescence of the NBD dye: Figure 5 shows the modulation of the fluorescence intensity of NBD by spiropyran moieties for three nanoparticle samples. After a NBD–nanoparticle complex dispersion was irradiated with UV light (300 nm, 15 W) for 15 minutes, it was immediately transferred to the fluorescence spectrometer to measure the emission (at an excitation wavelength of 490 nm). The characteristic fluorescence emission from NBD at 533 nm was significantly quenched and a new emission band at 635 nm appeared, which is the emission from the open-ring state of the spiropyran moiety. After irradiation with visible light (525 nm, 15 W LED lamp) for 20 minutes, the fluorescence intensity at 533 nm was restored (Figure 5).

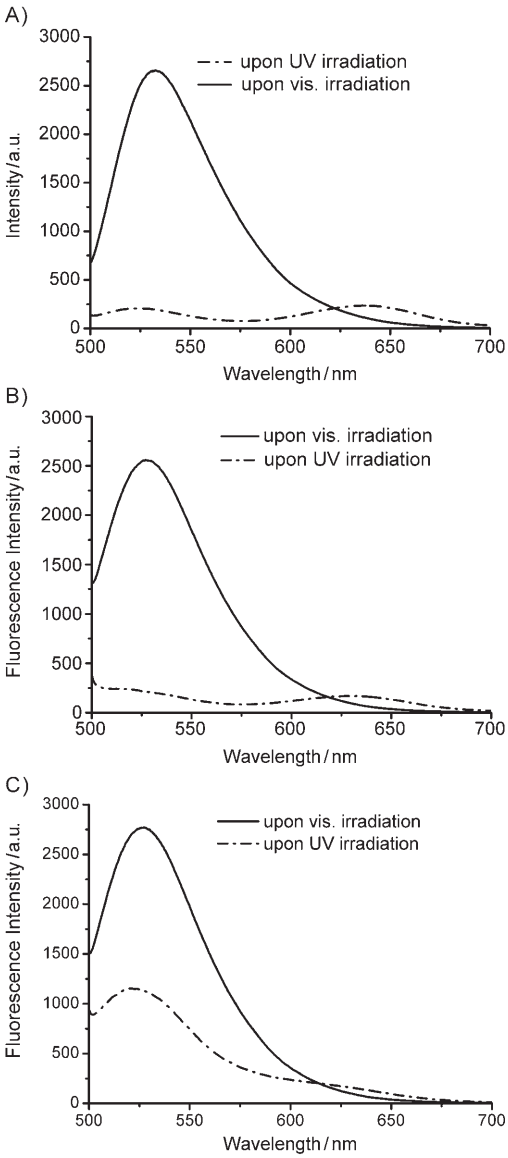

Figure 5. Fluorescence emission (excited at 490 nm, 25 °C) of NBD–nanoparticle complexes modulated by UV irradiation (300 nm) or by visible-light (525 nm) irradiation. The concentration of NBD is 1.07×10^{-5} M in aqueous dispersions and that of the spiropyran moiety is A) 1.2×10^{-3} (sample NP-A1, spiropyran feed: 0.10 g), B) 3.0×10^{-4} (sample NP-A3, spiropyran feed: 0.025 g), and C) 1.5×10^{-4} M (sample NP-A4, spiropyran feed: 0.0125 g), respectively.

For photoreversible fluorescence modulation using the dyad strategy,[28–30] the energy transfer process can be exploited to modulate the emissive behavior of the fluorophore–spiropyran (or other photochromes) dyads or triads as long as the emission band of the fluorophore and the absorption bands of the photochrome overlap significantly in one of the two states of the spiropyran fragment and the distance between the fluorophore (donor) and the spiropyran moiety (acceptor) is within the Förster radius (generally 1–10 nm).[31] Under these conditions, the photochemical transformation of the spiropyran can activate or suppress the transfer of the excitation energy from a fluorophore to a spiropyran moiety. For the dyad or triad systems, the distance between the energy donor and the acceptor can be controlled by inserting a spacer between them. These dyad or triad systems have the well-defined structure needed for effective energy transfer as well as good fluorescence modulation. However, a complicated synthetic process is required to prepare them. In this case, the emission band (500–650 nm) of the fluorophore NBD overlaps the absorption band (500–650 nm) of the McH state of the spiropyran in the nanoparticles. However, the SP state does not exhibit any absorption band in the emission band of NBD (500–650 nm), as shown in Figure 2. Thus, energy transfer from the excited state of NBD to the SP form of spiropyran is impossible, whereas energy transfer to the McH form is possible. From the perspective of an energy-level match, the energy of the first-excited singlet state of NBD was estimated to be 2.50 eV from the average frequencies of the absorption and emission bands ($\lambda_{max}=460$ nm, $\lambda_{em}=533$ nm). Similar calculations based upon absorption and emission maxima[12] gave a first-excited singlet-state energy of 3.65 eV ($\lambda_{max}=340$ nm) for the SP form of the spiropyran moiety in nanoparticles, and 2.05 eV ($\lambda_{max}=575$ nm, $\lambda_{em}=630$ nm) for the McH form of the spiropyran moiety. These data also indicate that energy transfer from NBD to the SP form of spiropyran is impossible, whereas that from NBD to the McH form is possible. Therefore, before ring-opening of the spiropyran moiety, no fluorescence quenching of NBD could be observed, whereas upon UV irradiation, the spiropyran moiety converts into the open-ring McH form and then the energy transfer from NBD to the McH form of spiropyran became efficient.

The energy-level match between the excited state of NBD and the McH form of spiropyran clearly indicates that the observed quenching of NBD fluorescence by the McH form arises through an energy transfer process. Förster's critical distances R_0 for this donor–acceptor pair in samples NP-A1, NP-A3, and NP-A4 have been calculated to be 43, 42, and 42 Å, respectively (see the Supporting Information). The slight differences in the R_0 values between the three samples may be due to different microenvironments in the different nanoparticle samples.[31] According to Förster's nonradiative energy transfer theory,[31,32] the energy transfer efficiency E, expressed by Equation (1), depends on R_0 and on the distance (r) between the donor (NBD) and the acceptor (McH). The energy transfer is effective over distances in the range of $R_0 \pm 0.5R_0$.[31] For NP-A1, this distance is $22 \leq r \leq 65$ Å.

$$E = \frac{R_0^6}{R_0^6 + r^6} \quad (1)$$

We used the sample NP-A1 to compare the effective energy transfer distance with the nanoparticle size. The measured average diameter of the core–shell nanoparticle is 82 nm, and according to the amount of shell (PEI) and core material (mainly PMMA) fed into the reaction medium, the average diameter of the hydrophobic core of this sample of nanoparticles can roughly be calculated to be 76 nm. In the core–shell nanoparticles, the NBD molecules (donor) reside in the core–shell interface, whereas the spiropyran moieties (acceptor) reside in the core. As the upper limit of the effective energy transfer distance in this sample is 65 Å (6.5 nm), an outer sphere of about 6.5 nm thickness, which represents about 43% of the overall volume of the hydrophobic core of the nanoparticle system, serves as the effective area[32] in which the McH form of the spiropyran can quench the fluorescence emission of NBD. In this regard, preparation of smaller nanoparticles can further increase the ratio of the effective volume in a nanoparticle.

Figure 5 also shows that, for the three samples (NP-A1, NP-A3, and NP-A4, with their average diameter of hydrophobic cores ranging from ca. 76 to ca. 90 nm), the amount of spiropyran moieties in the nanoparticle core can affect the energy transfer efficiency. We calculated the experimental energy transfer efficiency E between NBD and the McH form of spiropyran, the concentration of spiropyran in the dispersion (C_{SP}), the number of spiropyran moieties in one nanoparticle ($N_{SP/NP}$), and the average distance between the spiropyran moieties (D_{SP}) for the three samples (see Supporting Information) and listed them in Table 2.

Table 2. Characteristics of the three NBD–nanoparticle complexes samples.

Sample	C_{SP} [10^{-4} M]	D_{SP} [nm]	$N_{SP/NP}$	E	R_0 [Å]
NP-A1	12	3.56	13340	0.926	43
NP-A3	3.0	5.42	3470	0.917	42
NP-A4	1.5	6.84	1720	0.592	42

Based on the monomer feed ratio, for the three samples, each particle roughly contains on average 1720–13340 spiropyran moieties, which corresponds to a spiropyran-linked methacrylate (SPMA) feed of 0.0125–0.1 g (see the Experimental Section). The corresponding volume occupied by each spiropyran moiety is in the range of roughly 23–165 nm^3, or, on average, two spiropyran moieties are separated by a distance of around 3.56–6.84 nm. In this study, the NBD molecules were loaded into the nanoparticles at ambient temperature, which is far below the glass transition temperature of the hydrophobic core. Thus, most of the

NBD molecules cannot penetrate the inside of the cores and are located at the interface between the hydrophilic shell and the hydrophobic core. Based on the above estimation of the inter-spiropyran distance, at the higher spiropyran feed (for sample NP-A1 and NP-A3), there are plenty of spiropyran moieties located within the Förster radius of the NBD molecules at the interface between the hydrophilic shell and hydrophobic core. Therefore, upon UV irradiation, intraparticle energy transfer from the excited NBD dye to the McH state of the spiropyran moieties inside the nanoparticle core can take place. Thus the fluorescence emission of NBD was efficiently quenched (Figure 5). With a lower spiropyran feed (sample NP-A4), the fluorescence emission of NBD cannot be efficiently quenched, as illustrated in Figure 5C. For this NBD–nanoparticle sample, the measured energy transfer efficiency is only 0.59, and the calculated number of spiropyrans in the effective outer sphere is about 720, still more than that of NBD in one nanoparticle (ca. 120). We suppose one possible reason for the absence of quenching is that the spiropyran moieties are not homogeneously distributed in the hydrophobic cores of the nanoparticles.

The above results and discussions suggest that the photophysical theory can be applied to explain FRET in this core/shell nanoparticle system. However, the theory cannot accurately work for this system because its structure is much more complicated than those of unimolecule dyad systems, for example, the particle sizes of the different samples are not identical, the spiropyran moieties may not be homogeneously distributed in the particle cores, and short-range (less than 1 nm) interactions[31b] between donors (NBD) and acceptors (spiropyran) may exist.

Figure 6 shows a typical photoresponse of a NBD–nanoparticle complex in a water dispersion. Upon irradiation with 300 nm light, the fluorescence intensity gradually decreased over 20 min and then increased upon irradiation with 525 nm light, taking about 20 min for the complex to recover its fluorescence intensity. The switching of the fluorescence intensity of NBD is due to the photochemical conversion between the two states of the spiropyran moieties. The switching time is comparable to that of a polymer film incorporating spiropyran molecules,[33] but longer than that of spiropyran molecules in toluene or mineral oil solutions (tens of seconds to a few minutes).[34] The longer switching time may be due to the solid-state environment of the nanoparticles in which configurational switching must overcome energy barriers imposed by the closely packed organic molecules. In nonpolar or low-polar solutions, however, the barriers posed by fluidic solvent molecules may be much lower than those in the solid-phase core of the nanoparticles. Nonetheless, for some water-soluble spiropyran derivatives, the conversion from the McH form to the SP form is slow in water because high-polar solvent molecules tend to stabilize the zwitterionic McH form.[35] Recently, we developed a strategy for photoreversible fluorescence modulation by modification of β-cyclodextrin with spiropyran, and we used light to switch the fluorescence of rhodamine B (RhB) included in β-cyclodextrin.[36] However, the reversibility was only efficient in nonaqueous solution; the photochemical conversion from the McH form to the SP form took several hours in water. In this case, however, the spiropyran groups reside in the hydrophobic cores of the nanoparticles, in which the zwitterionic McH form cannot be stabilized by water, and the fluorescence intensity of NBD can be recovered much more quickly.

The reversible nature of the fluorescence modulation of the NBD–nanoparticle complexes upon exposure to alternating cycles of UV (300 nm) and visible-light (525 nm) illumination is illustrated in Figure 7 and in Table S1 of the Supporting Information. The visible light or UV can be applied to reversibly "turn on" and "turn off" the fluorescence of NBD. The appearance of an aqueous dispersion of NBD–nanoparticle complexes also reversibly changes on irradiation with UV or visible light, as shown in Figure S4 in the Supporting Information.

In Figure 7 and Table S1 in the Supporting Information, with repeated cycles of visible and UV irradiation, one can observe an increase in the fluorescence intensity of the "off state" (upon UV irradiation) and a decrease in the fluores-

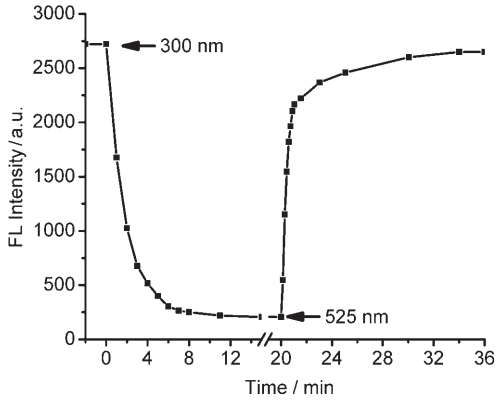

Figure 6. Fluorescence intensity (at 533 nm) changes of the NBD–nanoparticle (sample NP-A3) complex upon alternate irradiation with 300 nm UV and 525 nm visible light. The concentration of NBD in the dispersion is 1.07×10^{-5} M.

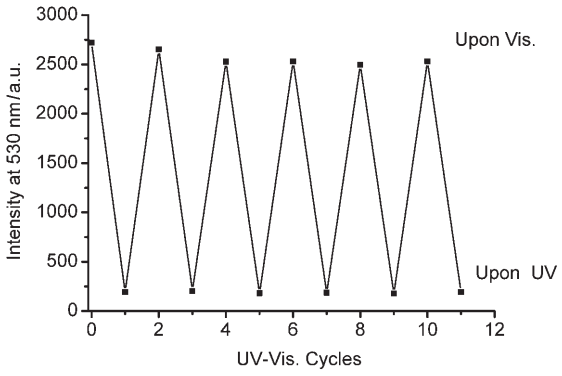

Figure 7. Fluorescence emission intensities for the NBD–nanoparticle complex in an aqueous medium (NBD concentration: 1.07×10^{-5} M, $\lambda_{ex}=$ 490 nm) recorded at 533 nm and 25 °C upon cycles of UV and visible-light irradiation.

cence intensity of the "on state" (upon visible-light irradiation), which indicates that some NBD molecules and spiropyran moieties undergo irreversible photodamage.[37] As a result of photodamage, the amount of intact NBD dye in the nanoparticles decreases. Thus the fluorescence intensity upon repeated visible-light irradiation is lower than the "on state" value observed upon the first visible-light irradiation. On the other hand, the amount of intact spiropyran moieties also decreases as a result of photodamage, and the remaining intact spiropyran (McH form) is not capable of quenching the fluorescence intensity of NBD to the "off state" value observed upon the first UV irradiation.

Conclusion

Amphiphilic core–shell nanoparticles containing spiropyran moieties have been prepared and they not only greatly enhance the fluorescence emission of the hydrophobic dye NBD in aqueous media, probably by accommodating the dye molecules in the interfaces between the hydrophilic shells and the hydrophobic cores, but also photoreversibly modulate the fluorescence of the dye through energy transfer. The hydrophobic core of the nanoparticles contains and protects the spiropyran moieties, whereas the hydrophilic shell allows the nanoparticles to be dispersed in water and forms an interface with the hydrophobic core to accommodate the hydrophobic dyes. This approach can be readily applied to other hydrophobic fluorophores (chromophores), thus opening up possibilities for their fluorescence modulation in aqueous media.

Experimental Section

Materials: Branched poly(ethyleneimines) (Acros), *tert*-butyl hydroperoxide (TBHP, Sigma), *N,N′*-dicyclohexylcarbodiimide (DCC, 99%, Alfa Aesar), 4-dimethylaminopyridine (DMAP, 99%, Alfa Aesar), 2,3,3-trimethylindolenine (Aldrich), 3-iodopropanoic acid (Aldrich), ethylene dimethacrylate (EDMA, Acros), and 5-nitrosalicylaldehyde (Aldrich) were used as received. Dichloromethane (DCM, A.R.) was washed with sulfuric acid and then distilled from CaH_2. 2-Hydroxyethyl methacrylate (HEMA, 97%, Aldrich) was dissolved in water (25 vol%) and washed four times with an equal volume of hexane, then dried with $MgSO_4$ and distilled under vacuum prior to use. The phenolic inhibitor in methyl methacrylate (MMA, Aldrich) was removed by washing three times with 10% sodium hydroxide solution and then with deionized water until the pH of the water layer was 7, and then it was further purified by vacuum distillation. Double-distilled water further purified with a Milli-Q system was used in this work. Tetrahydrofuran (THF, A.R.) was distilled over CaH_2. Petroleum ether, benzene, and other reagents were analytical reagents and used without further purification.

Synthesis of the carboxy-containing spiropyran (SPCOOH) and the spiropyran-linked methacrylate monomer (SPMA): During the synthesis, all the reaction vessels were wrapped in aluminum foil to ensure the reaction was performed in the dark. The carboxy-containing spiropyran l′-(β-carboxyethyl)-3′,3′-dimethyl-6–nitrospiro[indoline-2′,2-chromane] (referred to as SPCOOH) was synthesized as follows. 2,3,3-Trimethylindolenine (0.06 mol), 3-iodopropanoic acid (0.06 mol), and ethyl methyl ketone (5 mL) were heated under nitrogen at 100°C for 3 h. The resulting solid material was dissolved in water and the solution was washed with chloroform. Evaporation of water gave l-(β-carboxyethyl)-2,3,3-trimethylindolenine iodide (73% yield). This iodide (0.04 mol), 5-nitrosalicylaldehyde (0.04 mol), and piperidine (3.8 mL, 0.04 mol) were dissolved in ethyl methyl ketone, and the red solution was refluxed for 3 h. On standing overnight, the product precipitated as a yellow crystalline powder. This was filtered and washed with methanol to give the product SPCOOH (75% yield). The ^{1}H NMR spectrum of SPCOOH is shown in Figure S1 in the Supporting Information. ^{1}H NMR (400 MHz, deuterated DMSO, 25°C, TMS): $\delta = 1.0$–1.3 (6H; CH_3), 2.6 (2H; CH_2COO), 3.4–3.5 (2H; CH_2N), 5.9–6.0 (2H; olefinic protons), 6.6–8.2 (aromatic protons), 12.0 ppm (COOH, hydrogen-bonding).

For the synthesis of SPMA, SPCOOH (3.8 g, 10 mmol), HEMA (2.6 g, 20 mmol), and DMAP (0.272 g, 2 mmol) were added to a 100 mL round-bottomed flask equipped with a pressure-equalized dropping funnel, magnetic stirrer, and a nitrogen inlet. Dry THF (80 mL) was added to the flask and the solution was cooled to 0°C; a red-brown solution resulted. DCC (2.06 g, 10 mmol) was dissolved in dry THF (20 mL), and the solution was added to the SPCOOH/HEMA solution through the pressure-equalized dropping funnel over 45 min. The flask was maintained at 0°C for 2 h and then the temperature was raised gradually to 25°C over 24 h. The product was filtered with cold (0°C), dry THF (3×50 mL) to give a red filtrate. Then most of the solvent was evaporated from the filtrate under vacuum and the residue was washed with distilled water to give a red-purple precipitate. The precipitate was dissolved in benzene and filtered again. Afterwards, most of the solvent was evaporated, the solution was precipitated in a large amount of petroleum ether, and finally a fine red-purple precipitate of purified 2-[3-(3′,3′-dimethyl-6-nitrospiro[indoline-2′,2-chroman]-1′-yl)propanoyloxy]ethyl methacrylate (SPMA) was obtained. The target product was dried in a vacuum oven overnight at room temperature. The ^{1}H NMR spectrum of this product is shown in Figure S2 in the Supporting Information. ^{1}H NMR (400 MHz, $CDCl_3$, 25°C): $\delta = 1.0$–1.3 (6H; CH_3 of spiropyran), 1.8–1.9 (3H; CH_3 of HEMA, connected to olefinic carbon), 2.6–2.7 (2H; CH_2COO- of spiropyran), 3.5–3.6 (2H; CH_2N of spiropyran), 4.2 (4H; CH_2O of HEMA), 5.5–6.0 (4H; olefinic protons, CH_2 and 2 CH), 6.6–8.1 ppm (aromatic protons).

Synthesis of the spiropyran-based amphiphilic core/shell particles: Branched poly(ethyleneimine), with M_w of 1800, 10000, or 70000, respectively, was dissolved in water (75 mL) and then mixed with a mixture of purified MMA (3.0 g), ethylene dimethacrylate (EDMA, 0.03 g), and various amounts of SPMA (0.0125–0.1 g) in a three-necked flask equipped with a thermometer, a condenser, a magnetic stirrer, and a nitrogen inlet. The stirred mixture was purged with nitrogen for 30 min. The appropriate amount of TBHP was added and the mixture was heated at 80°C for 6 h under nitrogen. The product was filtered through a G2 sintered glass funnel. Then the colloid was centrifuged to remove residual water-soluble molecules, and the precipitate was recovered and dialyzed against water for 48 h. Finally an aqueous dispersion was obtained.

Synthesis and introduction of the NBD dye into nanoparticles in aqueous media: The NBD dye (NBD-C8) was synthesized and purified according to a literature procedure.[38] The prepared NBD dye was dissolved in dichloromethane to give a 10^{-4} M of solution. A given amount of the solution was transferred to a 25 mL flask and then the solvent was evaporated under vacuum. The same flask with the dried NBD dye was then filled with the aqueous dispersion of nanoparticles and the mixture was stirred for 48 h at 50°C to allow the dye molecules to move into the nanoparticles. Subsequently the mixture was cooled to room temperature.

Characterization: ^{1}H NMR spectra were recorded on a Bruker Avance 400 MHz NMR spectrometer. UV/Vis spectra were recorded on a Hitachi U-3010 UV/Vis spectrophotometer at room temperature. Fluorescence spectra were recorded on a Hitachi F-4500 Fluorescence spectrophotometer. Nanoparticle morphology was observed with a Seiko SII atomic force microscope (AFM) in the tapping mode at room temperature. The diameters of the nanoparticles were analyzed with a MALVERN Nano-ZS90 instrument. The diameters of the samples are the averaged values with a systematic (instrumental) error of around 5%. For the core–shell nanoparticle samples, the weight ratio of the shell

(PEI) to core material (PMMA and spiropyran) are known and thus, by assuming all the materials underwent reaction and were incorporated into the core–shell particles, the thickness of the shells and the diameters of the cores could be calculated with errors of about 5%.

Acknowledgement

This work was supported by the NSFC (Project Nos. 50573023, 50773022, 20534020 and 50473035), the GDNSF (Project No. 07006497), and the NCET.

[1] M. Bossi, V. Belov, S. Polyakova, S. W. Hell, *Angew. Chem.* **2006**, *118*, 7623; *Angew. Chem. Int. Ed.* **2006**, *45*, 7462.
[2] M. Irie, S. Kobatake, M. Hirochi, *Science* **2001**, *291*, 1769.
[3] a) A. Khan, S. Hecht, *Chem. Eur. J.* **2006**, *12*, 4764; b) S. Wu, J. Lu, F. Zeng, Y. Chen, Z. Tong, *Macromolecules* **2007**, *40*, 5060; c) S. Just, A. Aemissegger, P. Guntert, O. Zerbe, D. Hilvert, *Angew. Chem.* **2006**, *118*, 6445; *Angew. Chem. Int. Ed.* **2006**, *45*, 6297; d) R. Davis, N. Tamaoki, *Chem. Eur. J.* **2007**, *13*, 626.
[4] a) Y. Tian, C. Y. Chen, Y. J. Cheng, A. C. Young, N. M. Tucker, A. K. Y. Jen, *Adv. Funct. Mater.* **2007**, *17*, 1691; b) M. Zhu, L. Zhu, J. J. Han, W. Wu, J. K. Hurst, A. D. Q. Li, *J. Am. Chem. Soc.* **2006**, *128*, 4303.
[5] a) X. Guo, D. Zhang, D. Zhu, *Adv. Mater.* **2004**, *16*, 125; b) J. H. Cho, J. K. Hong, K. Char, F. Caruso, *J. Am. Chem. Soc.* **2006**, *128*, 9935.
[6] A. C. Benniston, A. Harriman, S. L. Howell, C. A. Sams, Y. G. Zhi, *Chem. Eur. J.* **2007**, *13*, 4665–4674.
[7] S. D. Straight, P. A. Liddell, Y. Terazono, T. A. Moore, A. L. Moore, D. Gust, *Adv. Funct. Mater.* **2007**, *17*, 777.
[8] a) L. M. Rossi, L. Shi, F. H. Quina, Z. Rosenzweig, *Langmuir* **2005**, *21*, 4277; b) X. G. Li, H. Li, M. R. Huang, *Chem. Eur. J.* **2007**, *13*, 8884; c) T. Deng, J. Li, J. H. Jiang, G. L. Shen, R. Q. Yu, *Chem. Eur. J.* **2007**, *13*, 7725; d) T. Zhang, J. L. Stilwell, D. Gerion, L. Ding, O. Elboudwarej, P. A. Cooke, J. W. Gray, A. P. Alivisatos, F. F. Chen, *Nano Lett.* **2006**, *6*, 800; e) A. Garcia-Bernab, M. Kramer, B. Olah, R. Haag, *Chem. Eur. J.* **2004**, *10*, 2822.
[9] a) S. J. Lim, B. K. An, S. D. Jung, M. A. Chung, S. Y. Park, *Angew. Chem.* **2004**, *116*, 6506; *Angew. Chem. Int. Ed.* **2004**, *43*, 6346; b) P. Teolato, E. Rampazzo, M. Arduini, F. Mancin, P. Tecilla, U. Tonellato, *Chem. Eur. J.* **2007**, *13*, 2238; c) J. K. Grey, D. Y. Kim, B. C. Norris, W. L. Miller, P. F. Barbara, *J. Phys. Chem. B* **2006**, *110*, 25569; d) L. Wang, Y. Li, *Chem. Eur. J.* **2007**, *13*, 4203; e) S. Si, T. K. Mandal, *Chem. Eur. J.* **2007**, *13*, 3160.
[10] a) O. S. Wolfbeis, *J. Mater. Chem.* **2005**, *15*, 2657; b) S. M. Buck, Y. E. L. Koo, E. Park, H. Xu, M. A. Philbert, M. A. Brasuel, R. Kopelman, *Curr. Opin. Chem. Biol.* **2004**, *8*, 540; c) A. Burns, P. Sengupta, T. Zedayko, B. Baird, U. Wiesner, *Small* **2006**, *2*, 723; d) Y. F. Cao, Y. E. L. Koo, R. Kopelman, *Analyst* **2004**, *129*, 745; e) F. Mancin, E. Rampazzo, P. Tecilla, U. Tonellato, *Chem. Eur. J.* **2006**, *12*, 1844; f) A. Mallick, M. C. Mandal, B. Haldar, A. Chakrabarty, P. Das, N. Chattopadhyay, *J. Am. Chem. Soc.* **2006**, *128*, 3126.
[11] a) P. C. Ray, G. K. Darbha, A. Ray, W. Hardy, J. Walker, *Nanotechnology* **2007**, *18*, 375504; b) J. Seelig, K. Leslie, A. Renn, S. Kuhn, V. Jacobsen, M. van de Corput, C. Wyman, V. Sandoghdar, *Nano Lett.* **2007**, *7*, 685; c) J. H. Kim, S. Chaudhary, M. Ozkan, *Nanotechnology* **2007**, *18*, 195105; d) F. M. Raymo, I. Yildiz, *Phys. Chem. Chem. Phys.* **2007**, *9*, 2036; e) M. Tomasulo, I. Yildiz, S. L. Kaanumalle, F. M. Raymo, *Langmuir* **2006**, *22*, 10284; f) M. Tomasulo, I. Yildiz, F. M. Raymo, *J. Phys. Chem. B* **2006**,*110*, 3853; g) I. L. Medintz, A. R. Clapp, F. M. Brunel, T. Tiefenbrunn, H. T. Uyeda, E. L. Chang, J. R. Deschamps, P. E. Dawson, H. Mattoussi, *Nat. Mater.* **2006**, *5*, 581; h) I. L. Medintz, A. R. Clapp, J. S. Melinger, J. R. Deschamps, H. Mattoussi, *Adv. Mater.* **2005**, *17*, 2450; i) A. R. Clapp, T. Pons, I. L. Medintz, J. B. Delehanty, J. S. Melinger, T. Tiefenbrunn, P. E. Dawson, B. R. Fisher, B. O'Rourke, H. Mattoussi, *Adv. Mater.* **2007**, *19*, 1921.
[12] a) M. P. Debreczeny, M. R. Wasielewski, S. Shinoda, A. Osuka, *J. Am. Chem. Soc.* **1997**, *119*, 6407; b) M. Tomasulo, I. Yildiz, F. M. Raymo, *Aust. J. Chem.* **2006**, *59*, 175; c) L. Song, E. A. Jares-Erijman, T. M. Jovin, *J. Photochem. Photobiol. A* **2002**, *150*, 177; d) L. Giordano, J. Macareno, L. Song, T. M. Jovin, M. Irie, E. A. Jares-Erijman, *Molecules* **2000**, *5*, 591; e) F. M. Raymo, M. Tomasulo, *Chem. Eur. J.* **2006**, *12*, 3186.
[13] a) W. W. Wu, A. D. Li, *Nanomedicine* **2007**, 2, 523; b) I. L. Medintz, H. T. Uyeda, E. R. Goldman, H. Mattoussi, *Nat. Mater.* **2005**, *4*, 435; c) E. Jares-Erijman, L. Giordano, C. Spagnuolo, K. Lidke, T. M. Jovin, *Mol. Cryst. Liq. Cryst.* **2005**, *430*, 257.
[14] C. D. Jones, J. G. McGrath, L. A. Lyon, *J. Phys. Chem. B* **2004**, *108*, 12652.
[15] L. Y. Zhu, W. W. Wu, M. Q. Zhu, J. J. Han, J. K. Hurst, A. D. Q. Li, *J. Am. Chem. Soc.* **2007**, *129*, 3524.
[16] S. Uchiyama, T. Santa, N. Okiyama, T. Fukushima, K. Imai, *Biomed. Chromatogr.* **2001**, *15*, 295.
[17] a) J. Xia, P. L. Dubin, "Protein-Polyelectrolyte complexes" in *Macromolecular Complexes in Chemistry and Biology* (Eds.: P. L. Dubin, J. Bock, R. M. Davies, D. N. Schultz, C. Thies), Springer, New York, **1994**, pp. 247–270; b) M. M. Andersson, R. Hatti-Kaul, *J. Biotechnol.* **1999**, *72*, 21.
[18] a) C. Rudolph, R. H. Muller, J. Rosenecker, *J. Gene Med.* **2002**, *4*, 66; b) S. P. Kasturi, K. Sachaphibulkij, K. Roy, *Biomaterials* **2005**, *26*, 6375; c) G. Backliwal, M. Hildinger, V. Hasija, F. M. Wurm, *Biotechnol. Bioeng.* **2008**, *99*, 721.
[19] a) B. C. C. Pessela, L. Betancor, F. Lopez-Gallego, R. Torres, G. M. Dellamora-Ortiz, N. Alonso-Morales, M. Fuentes, R. Fernandez-Lafuente, J. M. Guisan, C. Mateo, *Enzyme Microb. Technol.* **2005**, *37*, 295; b) T. Merdan, J. Callahan, H. Peterson, U. Bakowsky, P. Kopeckova, T. Kissel, J. Kopecek, *Bioconjugate Chem.* **2003**, *14*, 989.
[20] T. Iida, T. Mori, Y. Katayama, T. Niidome, *J. Controlled Release* **2007**, *118*, 364.
[21] a) M. Ero, H. Du, S. Sukhishvili, *Langmuir* **2006**, *22*, 11329; b) T. Ito, N. Iida-Tanaka, T. Niidome, T. Kawano, K. Kubo, K. Yoshikawa, T. Sato, Z. H. Yang, Y. Koyama, *J. Controlled Release* **2006**, *112*, 382.
[22] a) E. Lippert, W. Ludder, F. Moll, W. Nagele, H. Boos, H. Prigge, I. Seibold-Blankenstein, *Angew. Chem.* **1961**, *73*, 695; b) T. S. Singh, S. Mitra, *J. Lumin.* **2007**, *127*, 508; c) P. Borowicz, J. Herbich, A. Kapturkiewicz, J. Nowacki, *Chem. Phys.* **1999**, *244*, 251.
[23] a) B. Valeur, *Molecular Fluorescence: Principles and Applications*, Wiley-VCH, Weinheim, **2001**, pp. 200–225; b) J. R. Lakowicz, *Principles of Fluorescence Spectroscopy*, 3rd ed. Springer, New York, **2006**, pp. 205–235.
[24] A. Fissi, O. Pieroni, G. Ruggeri, F. Ciardelli, *Macromolecules* **1995**, *28*, 302.
[25] J. Xu, F. Zeng, S. Wu, C. Hou, X. Liu, Z. Tong, *Nanotechnology* **2007**, *18*, 265704.
[26] P. Li, J. Zhu, P. Sunintaboon, F. Harris, *Langmuir* **2002**, *18*, 8641.
[27] N. Shao, J. Y. Jin, S. M. Cheung, R. H. Yang, W. H. Chan, T. Mo, *Angew. Chem.* **2006**, *118*, 5066; *Angew. Chem. Int. Ed.* **2006**, *45*, 4944.
[28] C. C. Corredor, Z. L. Huang, K. D. Belfield, *Adv. Mater.* **2006**, *18*, 2910.
[29] J. L. Bahr, G. Kodis, L. Garza, S. Lin, A. L. Moore, T. A. Moore, D. Gust, *J. Am. Chem. Soc.* **2001**, *123*, 7124.
[30] T. Fukaminato, T. Sasaki, T. Kawai, N. Tamai, M. Irie, *J. Am. Chem. Soc.* **2004**, *126*, 14843.
[31] a) K. E. Sapsford, L. Berti, I. L. Medintz, *Angew. Chem.* **2006**, *118*, 4676; *Angew. Chem. Int. Ed.* **2006**, *45*, 4562; b) B. Valeur, *Molecular Fluorescence: Principles and Applications*, Wiley-VCH, Weinheim, **2001**, pp. 247–272.
[32] F. Gouanvé, T. Schuster, E. Allard, R. Méallet-Renault, C. Larpent, *Adv. Funct. Mater.* **2007**, *17*, 2746.
[33] M. Tomasulo, S. Giordani, F. M. Raymo, *Adv. Funct. Mater.* **2005**, *15*, 787.

[34] A. Shumburo, M. C. Biewer, *Chem. Mater.* **2002**, *14*, 3745.
[35] Y. Sheng, J. Leszczynski, A. A. Garcia, R. Rosario, *J. Phys. Chem. B* **2004**, *108*, 16233.
[36] S. Wu, Y. Luo, F. Zeng, J. Chen, Y. Chen, Z. Tong, *Angew. Chem.* **2007**, *119*, 7145; *Angew. Chem. Int. Ed.* **2007**, *46*, 7015.
[37] a) G. Baillet, G. Giusti, R. Guglielmetti, *J. Photochem. Photobiol. A* **1993**, *70*, 157; b) J. Foling, S. Polyakova, V. Belov, A. Blaaderen, M. L. Bossi, S. W. Hell, *Small* **2008**, *4*, 134; c) C. Eggeling, A. Volkmer, C. A. M. Seidel, *ChemPhysChem* **2005**, *6*, 791; d) G. S. Jiao, L. H. Thoresen, T. G. Kim, W. C. Haaland, F. Gao, M. R. Topp, R. M. Hochstrasser, M. L. Metzker, K. Burgess, *Chem. Eur. J.* **2006**, *12*, 7816.
[38] F. Bertorelle, R. Dondon, S. Fery-Forgues, *J. Fluorescence* **2002**, *12*, 205.

Received: December 18, 2007
Revised: March 3, 2008
Published online: April 9, 2008

